Heat Transfer Engineering, 21:34–43, 2000

0145–7632/00 $12.00 + .00

Theoretical Analysis and Experimental Investigation on Local Heat Transfer Characteristics of HFC-134a Forced-Convection Condensation inside Smooth Horizontal Tubes

PEI-WEN LI, MIN CHEN, and WEN-QUAN TAO

State Key Laboratory of Multi-Phase Flow in Power Engineering, School of Energy and Power Engineering, Xi'an JiaoTong University, Xi'an Shaanxi, People's Republic of China

An improved analysis model is presented for predicting the local heat transfer coefficient of forced condensation in the annular flow region inside smooth horizontal tubes. Heat transfer experiments for R-12 and R-134a are conducted inside a condensing tube with an inner diameter of 11 mm and a length of 13 m. The mass flux ranged from 200 to 510 kg/m^2 s, and the vapor qualities varied from 1.0 to 0.0. Compared with the experimental data, the numerical results have a deviation of not more than 20% and 25% for 80% of the total 47 points of R-12 and 88% of the total 226 points of R-134a, respectively.

In recent years, increasing attention has been paid to improving the performance of heat pump systems, refrigeration, and air-conditioning equipment. In the development of an improved system, an accurate prediction of its heat transfer characteristics in condenser is required. In many heat pump and refrigeration systems, the condensation process occurs inside horizontal tubes; thus, the analysis of heat transfer of forced-convective condensation inside horizontal tubes is of immense importance.

Pure analytical treatment of the two-phase flow during condensation is very difficult, if not impossible. This is partly because, during the condensation process, vapor quality progressively decreases along the flow direction, leading to different flow patterns at different locations. Among many flow patterns which may occur during condensation inside horizontal tubes, annular flow is the simplest pattern in flow configuration. On the other hand, many investigators have observed that

The work reported herein was supported by the National Planning Commission of China and the State Key Laboratory of Multi-Phase Flow in Power Engineering. The authors are also grateful to the help from Dr. J. P. Schirmann, ELF Altochem, France, in providing R134a.

Address correspondence to Wen-Quan Tao, State Key Laboratory of Multi-Phase Flow in Power Engineering, Xi'an JiaoTong University, Xi'an Shaanxi 710049, People's Republic of China. E-mail: wqtao@xjtu.edu.cn

for high vapor velocities, annular flow is the predominant flow pattern during condensation inside tubes, even for qualities as low as 25% [1–3]. This allows us to analyze the in-tube condensation problems based on the annular-flow configuration.

To predict forced condensation inside tubes, quite a few approximate models have been proposed in the literatures. A review of this subject may be found in [4]. The present studies of condensation inside horizontal tubes are based mainly on the model proposed by Carpenter and Colburn in 1951 [5]. This is basically because this model is relatively simple, while the approximations made are quite reasonable. The hypotheses adopted in this model are (1) due to the vapor shear, the flow in condensate layer is turbulent; (2) the major thermal resistance occurs in a laminar sublayer of the condensate film, and (3) the thickness of this layer can be calculated from generalized velocity distributions developed for single-phase flow in pipes.

A few authors, such as Reisbig and Liang [6], Azer et al. [7], Bae et al. [8], and Traviss et al. [9], made some analyses based on the above hypotheses. In their analyses, a flat plate was used to approximate a tube wall in solving the momentum equation for the condensate layer. We will discard this assumption.

The present analysis uses the von Karman equations of turbulent flow in pipes to represent the velocity distribution in the liquid film. In addition, the turbulent Prandtl number is used to link the governing momentum and energy equations. The agreement between the predicted results and our experimental data is satisfactory.

ANALYSIS

In this section, an approximate model will be adopted to derive an integral equation for predicting the local condensation heat transfer coefficient. The physical model of the problem is shown in Figure 1. As annular flow is considered, a uniform liquid layer thickness around the circumference of the tube is assumed to exist in the parameter ranges of interest. Entrainment of liquid droplet in the vapor will be neglected. Thus, the interface of vapor core and liquid layer is supposed to be smooth; and a steady, turbulent flow in the liquid film is assumed. The subcooling of the liquid film is neglected, and the liquid and vapor properties are taken to be constant and corresponding to its pressure. The static pressure is uniform across the tube, and axial diffusion is neglected.

Momentum and Energy Equations

Consider a differential element dz of the liquid film, with its outer radius being r as shown in Figure 1. The

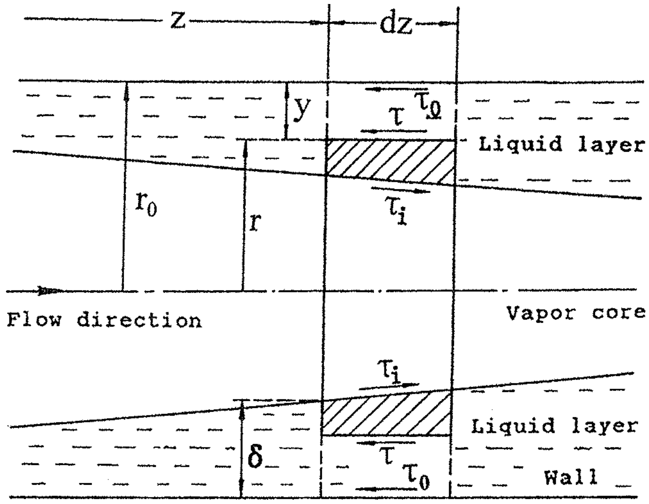

Figure 1 Annular flow condensation model.

momentum and heat transfer equations can be written as

$$\kappa = \rho_l(\nu_l + \varepsilon_m)\frac{dV_z}{dy} \tag{1}$$

$$\frac{Q}{A} = \rho_l Cp_l(a_l + \varepsilon_h)\frac{dT}{dy} \tag{2}$$

where A is the circumferential area of the element at the radius r. In an approximate analysis $\varepsilon_h/\varepsilon_m$ may be taken as a constant. Thus Eq. (2) can be written as

$$\frac{Q}{A} = \rho_l Cp_l(a_l + \mathrm{Pr}_t\,\varepsilon_m)\frac{dT}{dy} \tag{3}$$

where Pr_t is the ratio of eddy diffusivity ε_h to eddy viscosity ε_m and usually called turbulent Prandtl number. In this analysis the value of Pr_t is taken to be equal to 1.0 [7]. Integrating (3),

$$\int_0^{\delta} \frac{1}{A\rho_l Cp_l(a_l + \mathrm{Pr}_t\,\varepsilon_m)}\,dy = \int_{T_0}^{T_\delta} \frac{1}{Q}\,dT \tag{4}$$

The condensation heat transfer coefficient is defined as

$$h = \frac{Q}{A_0(T_\delta - T_0)} \tag{5}$$

Substitute Eq. (5) into Eq. (4), we get

$$\int_0^{\delta} \frac{A_0/A}{\rho_l Cp_l(a_l + \mathrm{Pr}_t\,\varepsilon_m)}\,dy = \frac{1}{h} \tag{6}$$

From Eq. (1), ε_m can be obtained:

$$\varepsilon_m = \frac{\kappa}{\rho_l (dV_z/dy)} - \nu_l \tag{7}$$

The shear stress velocity, $u_\kappa = \sqrt{\kappa_0/\rho_l}$, is used to define the following dimensionless velocity and length:

$$V_Z^+ = \frac{V_z}{u_\kappa} \qquad y^+ = \frac{y u_\kappa}{\nu_l} \tag{8}$$

Introducing V_Z^+ and y^+ into Eq. (7), ε_m can be written as

$$\varepsilon_m = \left[\frac{\kappa}{\rho_l u_\kappa^2}\left(\frac{1}{dV_z^+/dy^+}\right) - 1\right]\nu_l \tag{9}$$

and Eq. (6) can be expressed as

$$\frac{1}{h} = \int_0^{\delta^+} \frac{r_0^+/(r_0^+ - y^+)}{\rho_l C p_l (a_l + \mathrm{Pr}_t\ \varepsilon_m) u_\kappa} \nu_l\, dy^+ \tag{10}$$

where $r_0^+ = r_0 u_\kappa/\nu_l$ and $\delta^+ = \delta u_\kappa/\nu_l$.

The von Karman universal velocity distribution is used for the liquid layer, which is

$$0 < y^+ < 5 \qquad V_z^+ = y^+ \tag{11a}$$

$$5 \le y^+ < 30 \qquad V_z^+ = -3.05 + 5 \ln y^+ \tag{11b}$$

$$30 \le y^+ \qquad V_z^+ = 5.5 + 2.5 \ln y^+ \tag{11c}$$

Thus Eq. (9) can be written as

$$\varepsilon_m = \left(\frac{\kappa}{\kappa_0} - 1\right)\nu_l \qquad 0 < y^+ < 5 \tag{12a}$$

$$\varepsilon_m = \left(\frac{\kappa}{\kappa_0}\frac{y^+}{5} - 1\right)\nu_l \qquad 5 \le y^+ < 30 \tag{12b}$$

$$\varepsilon_m = \left(\frac{\kappa}{\kappa_0}\frac{y^+}{2.5} - 1\right)\nu_l \qquad 30 \le y^+ \tag{12c}$$

It can be seen from Eqs. (11) and (12) that in order to integrate Eq. (10), the expressions of κ/κ_0 and u_κ must be known. The expressions for κ/κ_0 will be derived from the momentum equation for a differential liquid film element, as shown in the following paragraph.

Evaluation of τ

The momentum equation for the shadowed part of the liquid film of the differential element dz in Figure 1 is

$$-\frac{dp}{dz}A_r + \kappa_i S_i - \kappa S = \left[\frac{d(U_l W_l)}{dz} - U_i \frac{dW_l}{dz}\right]\frac{A_r}{A_\delta} \tag{13}$$

where

$$A_r = \pi\left[(r_0 - y)^2 - (r_0 - \delta)^2\right]$$

$$A_\delta = \pi\left[r_0^2 - (r_0 - \delta)^2\right]$$

$$S_i = 2\pi(r_0 - \delta) \qquad S = 2\pi(r_0 - y)$$

Introducing the dimensionless parameters defined in Eq. (8), Eq. (13) can be written as follows:

$$\kappa = \frac{1 - \delta^+/r_0^+}{1 - y^+/r_0^+}\kappa_i - \frac{r_0}{2}\frac{dp}{dz}\left(1 - \frac{\delta^+}{r_0^+}\right)\left(\frac{1 - y^+/r_0^+}{1 - \delta^+/r_0^+} - \frac{1 - \delta^+/r_0^+}{1 - y^+/r_0^+}\right) + \frac{[(1 - y^+/r_0^+)^2 - (1 - \delta^+/r_0^+)^2]/[1 - (1 - \delta^+/r_0^+)^2]}{2\pi r_0 (1 - y^+/r_0^+)} \times \left[U_i \frac{dW_l}{dz} - \frac{d(U_l W_l)}{dz}\right] \tag{14}$$

where U_i is the vapor velocity at the interface of vapor and liquid film and is approximately equal to 1.25 U_l [10]. If y^+ is taken as zero, the above equation becomes the momentum equation for the whole differential element dz of the liquid film, and an expression for κ_0 can be obtained:

$$\kappa_0 = \left(1 - \frac{\delta^+}{r_0^+}\right)\kappa_i - \frac{r_0}{2}\frac{dp}{dz}\left(1 - \frac{\delta^+}{r_0^+}\right) \times \left[\frac{1}{1 - \delta^+/r_0^+} - (1 - \delta^+/r_0^+)\right] + \frac{1}{2\pi r_0}\left[U_i \frac{dW_l}{dz} - \frac{d}{dz}(U_l W_l)\right] \tag{15}$$

Rearranging Eq. (15), κ_i can be calculated:

$$\kappa_i = \frac{1}{1-\delta^+/r_0^+}\left\{\kappa_0 + \frac{r_0}{2}\frac{dp}{dz}\left(1-\frac{\delta^+}{r_0^+}\right)\right.$$
$$\times\left[\frac{1}{1-\delta^+/r_0^+}-\left(1-\frac{\delta^+}{r_0^+}\right)\right]$$
$$\left.-\frac{1}{2\pi r_0}\left[U_i\frac{dW_l}{dz}-\frac{d}{dz}(U_l W_l)\right]\right\} \tag{16}$$

It should be noted that in order to simplify Eq. (13), Bae et al. [8], Azer et al. [7], and Traviss et al. [9] used a flat plate to approximate a tube. Thus S and S_i in Eq. (13) were taken as equal in their analysis. This may be one of the reasons that Bae et al.'s numerical result had a serious deviation from their experimental data. Equations (14)–(16) show that, to integrate Eq. (10) numerically, expressions for κ_0, dp/dz, and δ^+ are necessary.

Evaluation of τ_0, dp/dz, *and δ^+*

The pressure gradient for two-phase flow in a tube may be expressed as the sum of two components if the gravity force is neglected for the horizontal orientation:

$$\frac{dp}{dz} = \left(\frac{dp}{dz}\right)_f + \left(\frac{dp}{dz}\right)_m \tag{17}$$

where

$$\left(\frac{dp}{dz}\right)_f = -\kappa_0\frac{S_0}{A_{r_0}} = -\kappa_0\frac{2}{r_0} \tag{18}$$

$$\left(\frac{dp}{dz}\right)_m = -\frac{1}{A_{r_0}}\frac{d}{dz}(U_v W_v + U_l W_l) \tag{19}$$

Using the Lockhart-Martinelli method, the frictional pressure gradient for two-phase flow can be related to the pressure gradient for vapor [9]:

$$\left(\frac{dp}{dz}\right)_f = \phi_v^2\left(\frac{dp}{dz}\right)_v \tag{20}$$

where

$$\left(\frac{dp}{dz}\right)_v = -0.09\frac{\mu_v^{0.2}G^{1.8}x^{1.8}}{\rho_v D^{1.2}}$$

and

$$\phi_v = 1 + 2.85X_{tt}^{0.523}$$

$$X_{tt} = \left(\frac{\mu_l}{\mu_v}\right)^{0.1}\left(\frac{1-x}{x}\right)^{0.9}\left(\frac{\rho_v}{\rho_l}\right)^{0.5}$$

Substituting $(dp/dz)_v$, ϕ_v, X_{tt} into Eq. (20), $(dp/dz)_f$ can be written as follows:

$$\left(\frac{dp}{dz}\right)_f = -0.09\left(\frac{\mu_v}{G_v D}\right)^{0.2}\frac{G_v^2}{D\rho_v}$$
$$\times\left\{1 + 2.85\left[\left(\frac{\mu_l}{\mu_v}\right)^{0.1}\left(\frac{1-x}{x}\right)^{0.9}\right.\right.$$
$$\left.\left.\times\left(\frac{\rho_v}{\rho_l}\right)^{0.5}\right]^{0.523}\right\}^2 \tag{21}$$

By using Eq. (21) and Eq. (18), κ_0 can be determined. For the acceleration term, $(dp/dz)_m$, the following apply:

$$U_l = \frac{(1-x)G}{\rho_l(1-\alpha)} \qquad U_v = \frac{xG}{\rho_v\alpha}$$

$$W_v = GA_{r_0}x \qquad W_l = GA_{r_0}(1-x)$$

where the local void fraction can be calculated using Zivi's equation [11],

$$\alpha = \frac{1}{1+[(1-x)/x](\rho_v/\rho_l)^{2/3}}$$

Thus $(dp/dz)_m$ can be calculated by the following equation:

$$\left(\frac{dp}{dz}\right)_m = -G^2\left[\frac{1-2x-2(1-x)(\rho_v/\rho_l)^{2/3}}{\rho_l(\rho_v/\rho_l)^{2/3}}\right.$$
$$\left.+\frac{2x+(1-2x)(\rho_v/\rho_l)^{2/3}}{\rho_v}\right]\frac{dx}{dz} \tag{22}$$

Substituting U_l, U_v, W_l, W_v into Eqs. (14) and (16),

$$\kappa = \frac{(1-\delta^+/r_0^+)}{(1-y^+/r_0^+)}\kappa_i - \frac{r_0}{2}\left(\frac{dp}{dz}\right)\left(1-\frac{\delta^+}{r_0^+}\right)$$
$$\times\left[\frac{(1-y^+/r_0^+)}{(1-\delta^+/r_0^+)}-\frac{(1-\delta^+/r_0^+)}{(1-y^+/r_0^+)}\right]$$
$$+\frac{1-y^+/\delta^+}{1-y^+/r_0^+}\left(\frac{\pi r_0 G^2}{2}\right)\left[\frac{1}{\rho_l(\rho_V/\rho_l)^{2/3}}\right]$$
$$\times\left\{1.25\left[x+(1-x)\left(\frac{\rho_v}{\rho_l}\right)^{2/3}\right]\right.$$
$$\left.+\left[1-2x-2(1-x)\left(\frac{\rho_v}{\rho_l}\right)^{2/3}\right]\right\}\frac{dx}{dz} \tag{23}$$

and

$$\kappa_i = \frac{1}{1-\delta^+/r_0^+}\left(\kappa_0 + \frac{r_0}{2}\left(\frac{dp}{dz}\right)\left[1-\left(\frac{1-\delta^+}{r_0^+}\right)^2\right]\right.$$

$$+\frac{\pi r_0 G^2}{2}\left[\frac{1}{\rho_l(\rho_v/\rho_l)^{2/3}}\right]$$

$$\times\left\{1.25\left[x+(1-x)\left(\frac{\rho_v}{\rho_l}\right)^{2/3}\right]\right.$$

$$\left.\left.+\left[1-2x-2(1-x)\left(\frac{\rho_v}{\rho_l}\right)^{2/3}\right]\right\}\frac{dx}{dz}\right) \qquad (24)$$

The next discussion will turn to how δ can be determined. For the differential element dz of liquid film,

$$G(1-x)\pi r_0^2 = \int_0^\delta \rho_l V_z\, 2\pi(r_0-y)\,dy \qquad (25)$$

Introducing the dimensionless velocity and length, the above equation can be written as

$$G(1-x)r_0^2 = \int_0^{\delta^+} \mu_l 2V_z^+\left(1-\frac{y^+}{r_0^+}\right)dy^+$$

Define Re_l as

$$\mathrm{Re}_l = \frac{G(1-x)2r_0}{\mu_l}$$

Then

$$\mathrm{Re}_l = \int_0^{\delta^+} 4V_z^+\left(1-\frac{y^+}{r_0^+}\right)dy^+ \qquad (26)$$

Substituting the equation for V_z^+ into Eq. (26), the relation between δ^+ and Re_l can be expressed by the following equations:

$$\mathrm{Re}_l = 2\delta^{+2} - \frac{4}{3}\frac{\delta^{+3}}{r_0^+} \qquad 0 < \delta^+ < 5 \qquad (27a)$$

$$\mathrm{Re}_l = 50.056 - \frac{41.807}{r_0^+} + \delta^+(20\ln\delta^+ - 32.2)$$

$$+\delta^{+2}\left(\frac{11.1}{r_0} - \frac{10}{r_0^+}\ln\delta^+\right) \quad 5 \le \delta^+ < 30 \qquad (27b)$$

$$\mathrm{Re}_l = -255.585 + \frac{2292.805}{r_0^+} + \delta^+(10\ln\delta^+ + 12)$$

$$-\frac{\delta^{+2}}{r_0^+}(8.5 + 5\ln\delta^+) \qquad 30 \le \delta^+ \qquad (27c)$$

From the above discussion it can be seen that once the quality x at a given location z is specified, along with the other parameters such as mass flux G and saturation properties at the condensing temperatures, the wall shear stress κ_0 and velocity u_κ as well as r_0^+ can be calculated. In order to derive δ^+ from Eq. (27), it is necessary to calculate the ranges of Re_l at a given r_0^+ when δ^+ varies from 0 to 5, 5 to 30, and above 30. Next the approximate equation for δ^+ can be selected from Eq. (27) according to the value of Re_l at a given location of z.

Numerical Procedure

The numerical integration of Eq. (10) proceeds as follows:

1. Use Eqs. (18) and (21) to calculate δ_0 and u_κ, then solve for δ^+ from Eq. (27).
2. Use Eqs. (21) and (22) to evaluate dp/dz.
3. To calculate κ_i and κ, use Eqs. (24) and (23).
4. With the calculated value of κ and κ_0, integrate Eq. (10) to obtain the value of h.

EXPERIMENT

A test rig was built for conducting the condensation heat transfer experiment (Figure 2), which consisted of a closed-loop refrigerant flow circuit driven by a magnetic force-driven pump and a cooling-water supplying system. The test section was a double-pipe counterflow heat exchanger, in which the refrigerant flowed inside the inner copper tube, with an inner diameter of 11 mm and a wall thickness of 2 mm, and the cooling water flowed countercurrently in the outer stainless steel annulus, with an inner diameter of 24 mm. The total 13-m-long test section was made up of five straight sections and four turns. The outer annulus of each straight section was subdivided into two subsections. Thus the whole test section had 10 subsections which rendered the local and average heat transfer coefficients to be measured. To have an inlet condition of $x = 1$, a preheater was used. The vapor superheating was controlled in the range of 2–3°C, and the sensitive heat was neglected in the energy balance computation.

The condensation heat transfer rate was measured at individual subsections with a length of 1.3 m each.

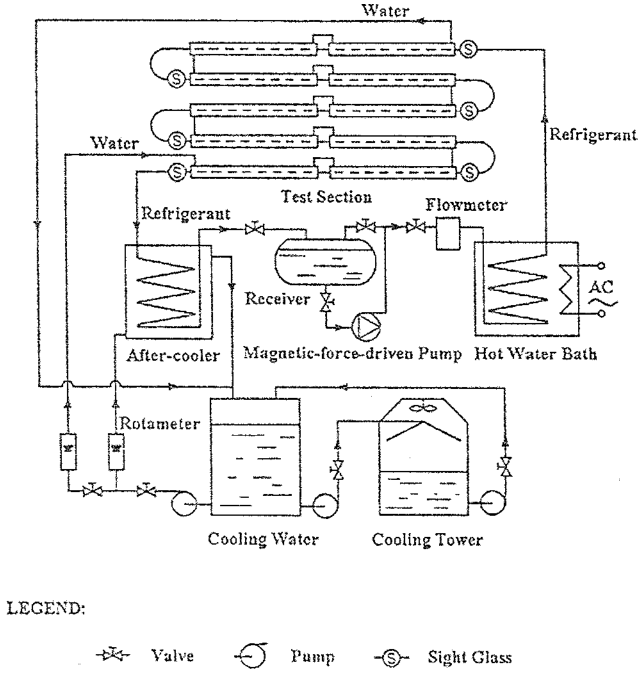

Figure 2 Schematic diagram of test facility.

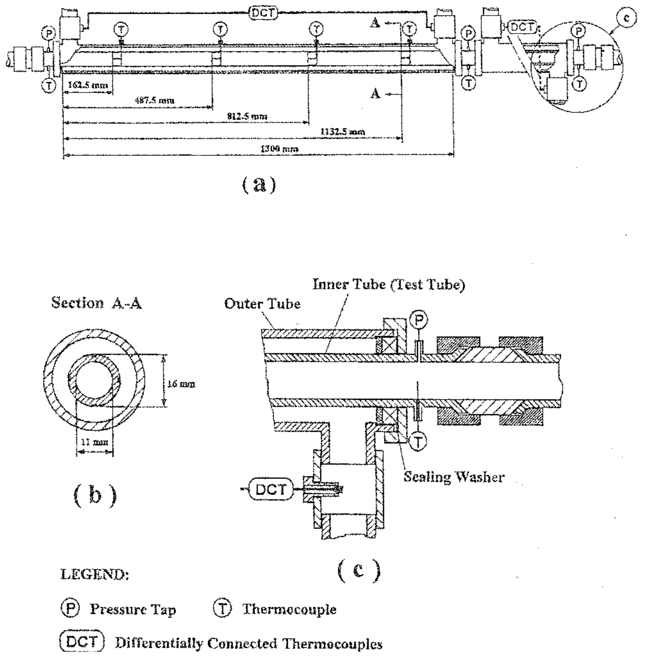

Figure 3 Details of test section.

Differentially connected thermocouples were installed at the inlet and outlet of each subsectional annulus for measuring the temperature rise of the water passing through it, and the overall temperature rise was also checked against the sum of the individual temperature increases. At four axial locations of each subsection, 16 thermocouples were soldered flush to the outside surface of the inner tube to measure the wall temperature; and the arithmetic mean of the 16 thermocouple readings was taken as the average wall temperature of the subsection (Figure 3). The inner tube of each subsection was instrumented with two thermocouples and pressure taps to measure the temperature and pressure of refrigerants. Six pieces of sight glass were set up in the test rig, with two located at the beginning and end of the entire test tube and the other four situated between each two subsections sequentially.

A positive-displacement flow meter was used to measure the flow rate of refrigerant. The refrigerant pressure was measured using a pressure gauge accurate to 6.25 kPa. The water flow rate was measured by a rotameter and by weighing the total mass of water passed in a time span. The calibrated thermocouples were 0.15 mm in diameter and had an uncertainty of ±0.30°C for temperature measurement.

An overall heat balance was performed for each run by comparing the heat gained by the water with the heat released by the refrigerant in the entire test section. For all runs, the energy balance agreed within ±8%.

Condensation experiments on R-12 and R-134a were performed under the following conditions: mass flux from 200 to 510 kg/m^{2}s, condensing temperature from 27 to 35°C, pressure from 0.716 to 0.886 MPa, vapor quality from 1.0 to 0.0, and heat flux from 4.0 to 28.0 kW/m^2.

The uncertainty analysis method suggested by Kline and McClintock [12] was used to estimate the experimental uncertainty. For the condensation of R-12 and R-134a, the uncertainty in the heat transfer coefficient was about ±6.8%. The thermodynamic properties of R-134a and R-12 used in this work are from [13, 14].

RESULTS AND DISCUSSION

Quality Variation Pattern along Flow Direction

As indicated earlier, the vapor quality progressively changes as condensation occurs along the flow direction, and it is an important parameter in predicting the local condensation heat transfer coefficient. In our experiments, the local average value of vapor quality for each subsection was determined. The variation of this vapor quality along the flow direction is shown in Figures 4 and 5 for 50 runs of R-134a and 10 runs of R-12, respectively, where L is the total length between $x = 1.0$ and $x = 0.0$. For the dashed lines in Figures 4 and 5, the quality gradients were assumed to be constant, that is, $dx/dz = -1/L$.

As can be seen from Figures 4 and 5, the overall variation trend for different runs of each medium is quite consistent, although minor scatter exists and a darkened area is used to represent the overall variation pattern. It is

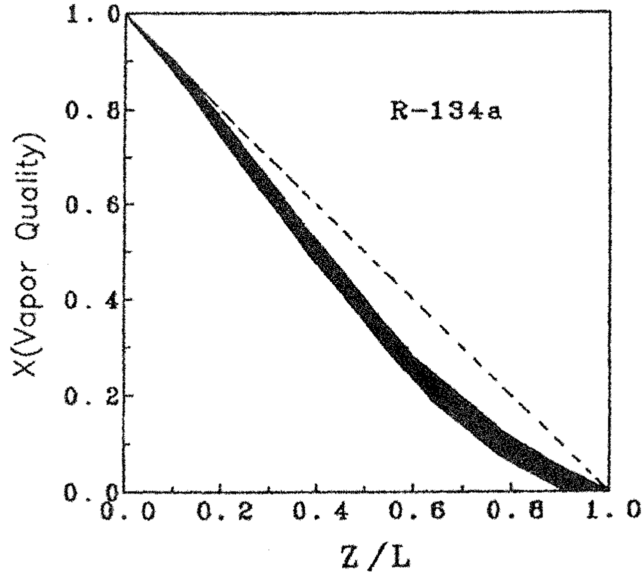

Figure 4 Variation of vapor quality along flow direction (R-134a).

also interesting to note that the quality variation pattern of the present study agrees quite well with most results provided in previous works as summarized in [15].

Using the experimental data, two equations for determining the average vapor quality against dimensionless length z/L are fitted as follows.

For R-12,

$$x = 1 - 1.13207\left(\frac{z}{L}\right) - 0.545664\left(\frac{z}{L}\right)^2 + 0.677734\left(\frac{z}{L}\right)^3 \quad (28)$$

For R-134a,

$$x = 1 - 1.24146\left(\frac{z}{L}\right) - 0.417106\left(\frac{z}{L}\right)^2 + 0.658566\left(\frac{z}{L}\right)^3 \quad (29)$$

The average deviations of these two fittings are about 7% and 12%, respectively, with larger scatters in the low-quality region. These two equations were adopted in the numerical integration of Eq. (10) to obtain the local average value of h.

Comparison between Predicted and Measured Results

The predicted and measured data of the local average condensation heat transfer coefficients are shown in Figures 6–8. Both numerical and experimental results show that condensation heat transfer coefficient inside the tube decreases with decreasing vapor quality. It can be seen that the agreement between the predicted and measured results is satisfactory if the vapor qualities are above 0.4. In the ranges of tested mass flux, the qualities corresponding to the restriction of annular flow are approximately above 0.4 or 0.5. This explains why the predicted heat transfer coefficients deviate from the experimental data dramatically when the qualities are below 0.4. The theoretical analysis assumed a smooth and symmetrical interface between vapor core and liquid film; however, the wave and nonsymmetrical effects

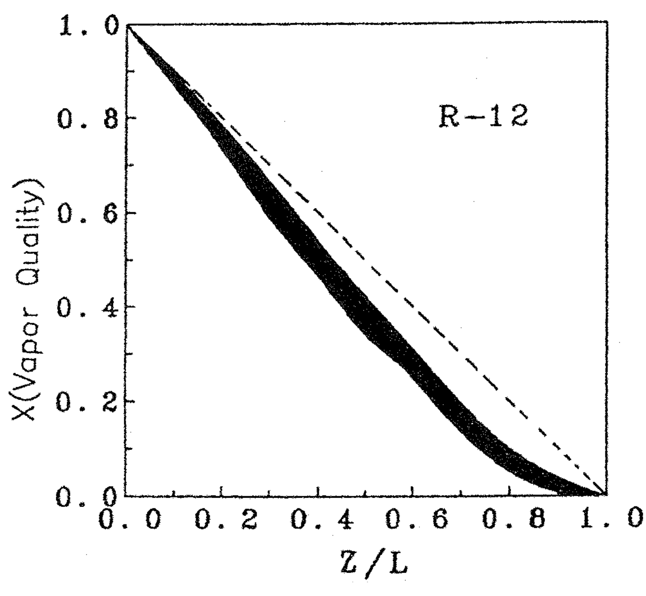

Figure 5 Variation of vapor quality along flow direction (R-12).

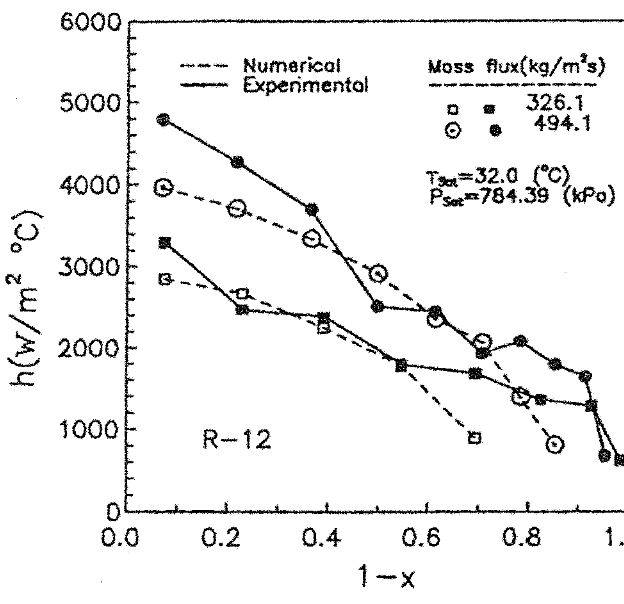

Figure 6 Local average heat transfer coefficient (R-12).

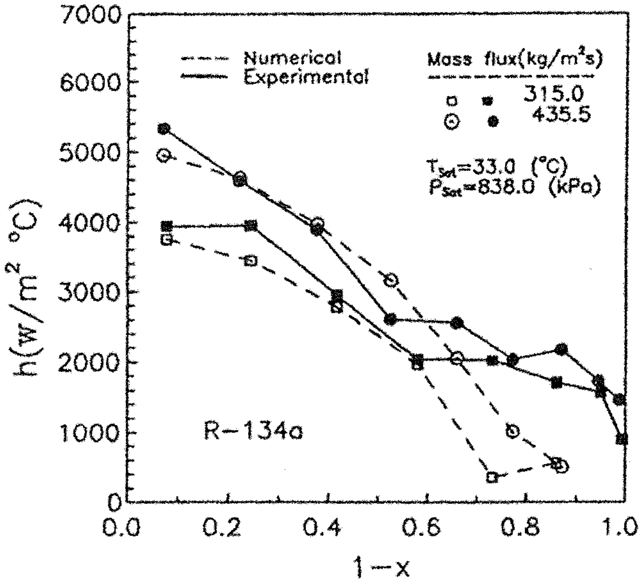

Figure 7 Local average heat transfer coefficient (R-134a, $T_{\text{sat}} = 33°\text{C}$).

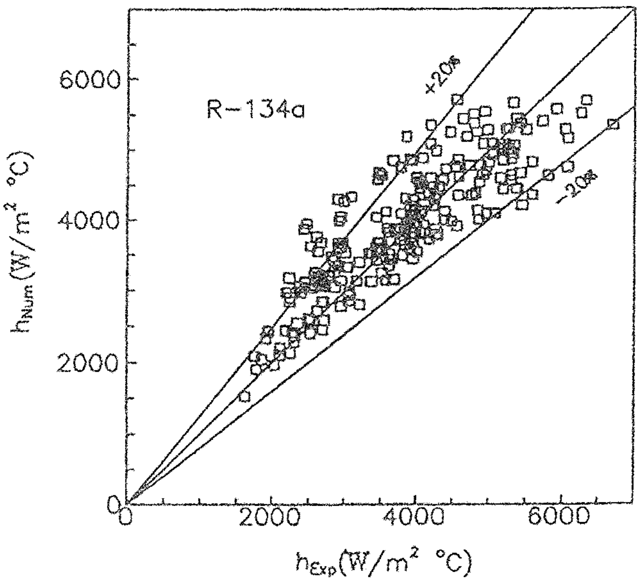

Figure 9 Comparison of predicted and measured heat transfer coefficient (R-134a).

of the interface, which occur in the low-quality region, may significantly increase the heat transfer performance. For the annular flow region with x larger than 0.4, the theoretical predictions agree with the experimental results quite satisfactorily, with 83% of the 47 predicted heat transfer data of R-12 deviating from the experimental results within ±20% and 88% of the 226 predicted data of R-134a deviating within ±25%. The largest deviations of heat transfer coefficients between predicted and experimental data are not over ±31% and ±35% for R-12 and R-134a, respectively, as shown in Figures 9 and 10.

Comparison between the New Analysis and That of Bae et al. [8]

The predictions by the method of Bae et al. and the new analysis are shown in Figures 11 and 12 along with the experimental data. Apparently, the predicted results by the new analysis have better agreement than that by Bae et al.'s method if annular flow is considered (i.e., $x > 0.4$). The reason for this has been mentioned in the above discussion.

In our numerical prediction, Eqs. (28) and (29) were used to determine the local vapor quality. However,

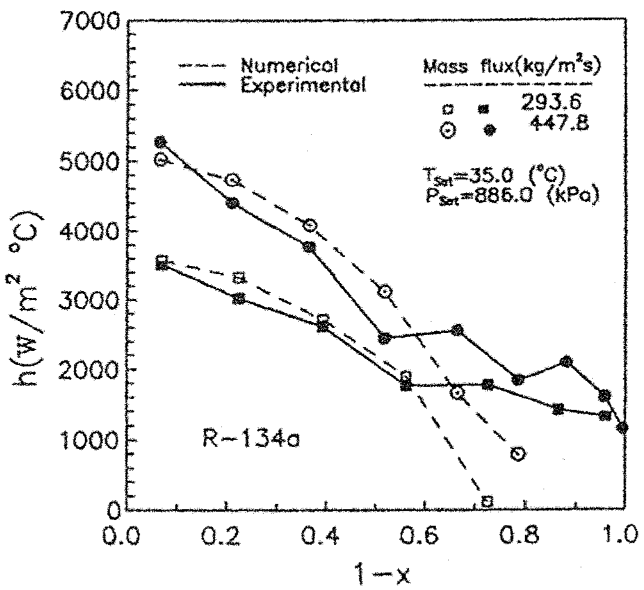

Figure 8 Local average heat transfer coefficient (R-134a, $T_{\text{sat}} = 35°\text{C}$).

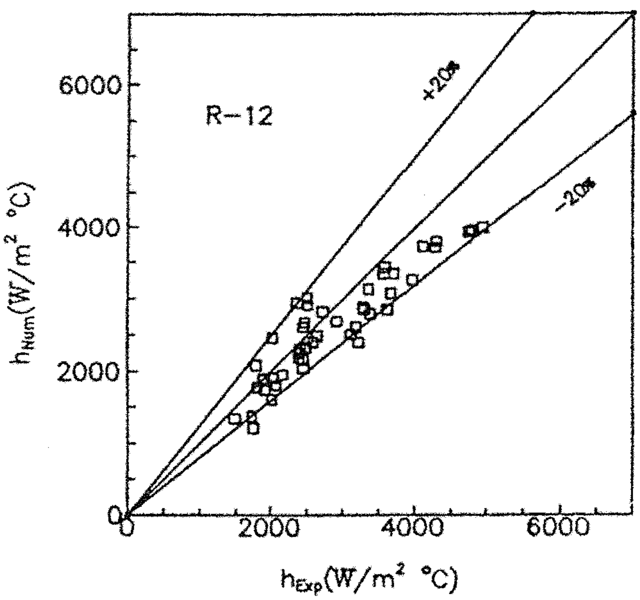

Figure 10 Comparison of predicted and measured heat transfer coefficient (R-12).

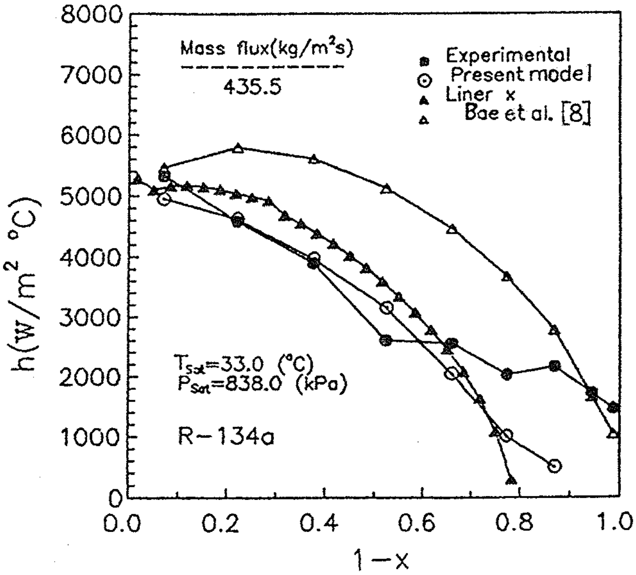

Figure 11 Comparison of predicted heat transfer coefficient using different models with measured data (R-134a).

in many practical cases, this vapor quality distribution equation may not be known a priori. It is interesting to check the sensibility of local heat transfer coefficient distribution to the vapor quality distribution. A natural and simple assumption is that the vapor quality is linearly distributed along the flow direction; that is, the value of dx/dz is adopted as constant, $-1/L$. The numerical results using this simple assumption are shown by the dashed lines in Figures 11 and 12. It can be seen that the difference between the predicted heat transfer coefficients is not considerable for R-12 and R-134a. Thus the uniform value of $dx/dz = -1/L$ is a good approximation in predicting the heat transfer coefficient

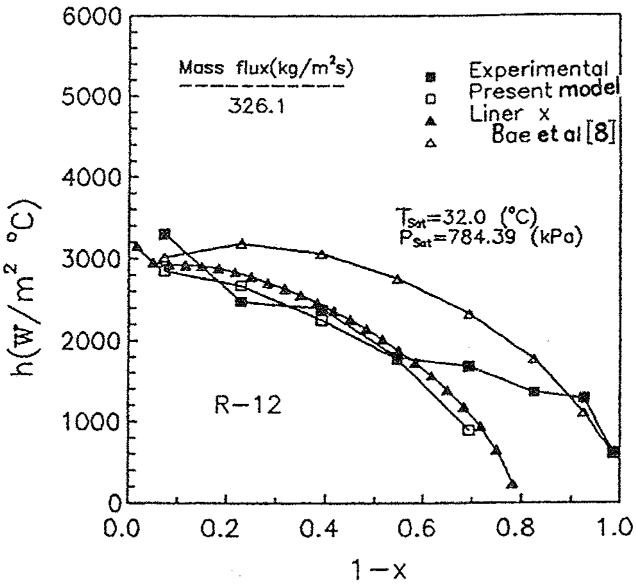

Figure 12 Comparison of predicted heat transfer coefficient models with measured data (R-12).

for annular flow by the present analysis if measured data are not available.

CONCLUSIONS

In this work, an experimental study on forced-convective condensation heat transfer inside a horizontal tube was conducted for R-12 and R-134a in the mass flux range from 200 to 510 kg/m^2 s. By directly measuring the wall temperature of the subsection condensing tube and the local heat transfer rate, a total of 273 local average condensation heat transfer coefficients and corresponding vapor qualities were obtained. Two empirical equations for determining the vapor quality along the flow direction were fitted for R-12 and R-134a.

An improved analysis model for numerical predicting the local heat transfer coefficient in the annular flow region was presented, into which von Karman's law of universal velocity distribution in a circular tube, and the Lockhart-Martinelli method for determining the two-phase flow pressure drop were incorporated. The agreement between the predicted and measured local average condensation heat transfer coefficient was quite satisfactory in the region of vapor quality from 0.4 to 1.0. It was found that the predicted local average condensation heat transfer coefficient was not very sensitive to the vapor quality distribution along the flow direction, and a uniform vapor quality gradient may be considered as a good approximation.

NOMENCLATURE

a_l thermal diffusivity, m^2/s
A circumferential area ($= 2\pi r\, dz$), m^2
A_0 circumferential area of inner wall of tube ($= 2\pi r_0\, dz$), m^2
A_r cross-sectional area of liquid film at r, m^2
A_δ cross-sectional area of whole liquid film, m^2
A_{r_0} cross-sectional area of tube at inner side, m^2
Cp_l saturated liquid specific heat, J/kg°C
D inner diameter of condensing tube, m
G mass flux based on cross-sectional area, kg/m^2 s
h heat transfer coefficient, W/m^2°C
L total length of condensation, m
p pressure, N/m^2
Pr_t turbulent Prandtl number ($= \varepsilon_h/\varepsilon_m$)
Q heat, W
r radius, m
Re_l Reynolds number of liquid [$= G(1 - x)2r_0/\mu_l$, based on inner diameter of tube]
S perimeter, m
T temperature, °C
T_δ saturation temperature, °C

u_κ friction velocity (defined as $u_\kappa = \sqrt{\kappa_0/\rho_l}$), m/s
U averaged axial velocity, m/s
V_z local axial velocity, m/s
W mass flow rate, kg/s
x vapor quality
y distance from tube wall, m
z axial distance from condenser inlet, m
α void fraction
δ thickness of the condensate film, m
ε_h eddy diffusivity, m^2/s
ε_m eddy viscosity, m^2/s
μ dynamic viscosity, kg/m s
ν kinematic viscosity, m^2/s
ρ density, kg/m^3
κ shear stress, N/m^2
ϕ_v parameter used in Lockhart-Martinelli method
X_{tt} Lockhart-Martinelli parameter

Subscripts

f friction
i liquid–vapor interface
l liquid
m mass acceleration term
sat saturation
v vapor
z local value
0 wall

Superscripts

+ dimensionless value

REFERENCES

[1] Traviss, D. P., and Rohsenow, W. M., Flow Regimes in Horizontal Two-Phase Flow with Condensation, *ASHRAE Trans.*, vol. 79, part 2, pp. 31–39, 1973.
[2] Tandon, T. N., Varma, H. K., and Gupta, C. P., A New Flow Regimes Map for Condensation inside Horizontal Tubes, *ASME J. Heat Transfer*, vol. 104, no. 3, pp. 763–768, 1982.
[3] Breber, G., Palen, J. W., and Tabork, J., Prediction of Horizontal Tubeside Condensation of Pure Components Using Flow Regime Criteria, *ASME J. Heat Transfer*, vol. 102, no. 3, pp. 471–476, 1980.
[4] Marto, J. P., Heat Transfer in Condensation, in S. Kakac (ed.), *Boilers, Evaporator, and Condensers*, pp. 512–570, Wiley, New York, 1991.
[5] Carpenter, F. G., and Colburn, A. P., The Effect of Vapor Velocity on Condensation inside Tubes, in *General Discussion of Heat Transfer, The Institute of Mechanical Engineers and ASME*, pp. 20–26, July 1951.
[6] Reisbig, R. L., and Liang, C. Y., Prediction of Heat Transfer from Condensing Refrigerant 12, *ASHRAE Trans.*, vol. 77, part 1, pp. 202–209, 1971.
[7] Azer, N. Z., Abis, L. V., and Soliman, H. M., Local Heat Transfer Coefficients during Annular Flow Condensation, *ASHRAE Trans.*, vol. 78, part 2, pp. 135–143, 1972.
[8] Bae, S., Maulbetsch, J. S., and Rohsenow, W. M., Refrigerant Forced-Convection Condensation inside Horizontal Tubes, *ASHRAE Trans.*, vol. 78, part 1. pp. 104–116, 1972.
[9] Traviss, D. P., Rehsenow, W. M., and Baron, A. B., Forced-Convection Condensation inside Tubes: A Heat Transfer Equation for Condenser Design, *ASHRAE Trans.*, vol. 79, part 1, pp. 157–165, 1973.
[10] Soliman, H. M., Schuster, J. R., and Bernson, P. J., A General Heat Transfer Correlation for Annular Flow Condensation. *Trans. ASME Ser. C*, vol. 90, no. 2, pp. 267–276, 1968.
[11] Zivi, S. M., Estimation of Steady State Steam Void-Fraction by Means of the Principle of Minimum Entropy Production, *Trans. ASME, Ser. C*, vol. 86, no. 2, pp. 237–252, 1964.
[12] Kline, S. J., and McClintock, F. A., Describing Uncertainties in Single-Sample Experiments, *Mech. Eng.*, vol. 75, pp. 3–8, 1953.
[13] ASHRAE, *Fundamentals*, American Society of Heating, Refrigeration, and Air Conditioning Engineers, Atlanta, GA, 1994
[14] ASHRAE, *Fundamentals*, American Society of Heating, Refrigeration, and Air Conditioning Engineers, Atlanta, GA, 1995.
[15] Shah, M. M., A General Correlation for Heat Transfer during Film Condensation inside Pipes, *Int. J. Heat Mass Transfer*, vol. 22, pp. 547–556, 1979.

Pei-Wen Li received his bachelor's degree in Nuclear Engineering in 1988 from Xi'an Jiaotong University of China. He continued his study in the same university and received his M.S. and Ph. D. degrees in Energy and Power Engineering in July 1991 and March 1995, respectively. Then he was employed as a lecturer at the same university. His research covers numerical heat transfer and fluid flow, heat/mass transfer of jet impingement flow, natural convection, boiling and condensation heat transfer of new refrigerants, and turbulence drag reduction.

Min Chen received his B.S. from Huazhong University of Science and Technology, China, M.S. from Tianjin University, China, and Ph.D. from Xi'an Jiaotong University, China. He is currently a Lecturer in the Engineering Mechanics Department at Tsinghua University, Beijing, China. His areas of interest are boiling and condensation heat transfer, thermodynamic properties of fluids, thermal-related molecular dynamics, and Monte Carlo simulations.

Wen-Quan Tao is a Professor of Engineering Thermophysics at the Xi'an Jiaotong University, Xi'an, China. He graduated from Xi'an Jiaotong University in 1962 and received his graduate diploma from the same university in 1966. He has written over 120 journal articles and conference papers in the areas of numerical heat transfer, enhancement of convective heat transfer, phase-change heat transfer of alternatives, and natural convection in enclosures with isolated internal bodies. He is also the author or co-author of six textbooks on heat transfer and numerical heat transfer.